Toward the catalytic synthesis of phosphiranes. A computational study

T.P.M. Goumans, Andreas W. Ehlers, Koop Lammertsma *

Department of Organic and Inorganic Chemistry, Faculty of Sciences, Vrije Universiteit, De Boelelaan 1083, NL-1081 HV, Amsterdam, The Netherlands

Abstract

Reaction pathways for the formation of zirconocene phosphinidene complex $Cp_2Zr(PR_3){=}PR$ from Cp_2ZrCl_2 and LiH and LiPRH and its reactivity to 1,2-dichloroethane are explored with density functional theory using model structures that are devoid of substituents. After the initial $Cp_2Zr(Cl)PH_2$ is generated with $LiPH_2$ reaction with LiH is likely to eliminate HCl in a single step to give directly the 16-electron complex $Cp_2Zr{=}PH$, which is stabilized by the PH_3 phosphine ligand. The intermediate formation of a phosphine hydride complex, $Cp_2Zr(H)PH_2$ resulting from hydride substitution, is unlikely both on the basis of unfavorable reaction energies and calculated ^{31}P NMR chemical shifts that indicate that such a species cannot have been observed experimentally. It is likely that a diphosphine complex, $Cp_2Zr(PH_2)_2$, results on using an excess of the lithium phosphide, which on H-transfer gives directly the phosphine-stabilized phosphinidene complex. The reactivity of this species is dominated by the release of its stabilizing phosphine ligand to give a highly reactive 16-electron phosphinidene complex, $Cp_2Zr{=}PH$, which reacts with 1,2-dichloroethane after coordination to one of the chlorine atoms in two asynchronous metathesis steps to the three-membered phosphirane ring. In this process, $ZrCl_2$ is reformed enabling its recycling to regenerate the phosphinidene complex. This study highlights the special reactivity of the 16-electron $Cp_2Zr{=}PH$ and suggests that related complexes may be generated similarly, thereby expanding the synthetic potential of these nucleophilic reagents.
© 2005 Elsevier B.V. All rights reserved.

Keywords: Zirconium complexes; σ-Bond metathesis; Catalysis; Phosphinidenes; DFT calculations; Phosphiranes

1. Introduction

Transition metal complexed phosphinidenes are versatile reagents [1]. Their properties parallel those of the carbenes [2], and likewise [3] they can be classified according to their reactivity as electrophilic (Fischertype) [4] or nucleophilic (Schrock-type) [5], yet their chemistry is still much less developed. The *electrophilic* phosphinidenes are transient reactive intermediates that are generated in situ by cheletropic elimination from 7-phosphanorbornadiene [6] or phosphirane [7] in the presence of an electron-rich trapping reagent such as an alkene, alkyne, carbonyl, imide, alcohol, or amine [1]. Recently, the group of Carty reported stable phosphinidene cations ($[L_nM{=}PR]^+$) that are isolable [8]. Most neutral *nucleophilic* phosphinidene complexes are also stable and crystalline. One actinide and several early transition metal phosphinidene complexes have been prepared since the early 1980s [9,10], while those with late transition metal groups are of more recent vintage [11]. Their reactivity, which differs distinctly from those that are electrophilic, has hardly been explored [1–3,12].

Only zirconium phosphinidene complex **1**, developed by Stephan and coworkers, has been studied in some detail [10]. The oxo- and halophilicity of the zirconium metal combined with the nucleophilicity of the phosphorus atom makes this complex reactive toward carbon–oxygen

* Corresponding author. Tel.: +31 20 598 7474; fax: +31 20 598 7488.
  E-mail address: K.Lammertsma@few.vu.ml (K. Lammertsma).

and carbon–halogen bonds to yield phosphaalkenes and phosphorus heterocycles (Scheme 1) [10]. The active species is assumed to be the 16-electron phosphinidene Cp$_2$Zr=PMes* that is formed upon dissociation of the labile trimethylphosphine ligand [10,11c].

Most nucleophilic 18-electron phosphinidene complexes are less reactive than **1** due to their protecting bulky ligands and substituents, and the high dissociation energy for the stabilizing two-electron σ-donor ligand [11c]. In those cases where the stabilizing ligand is absent, dimers of the 16-electron species are obtained [11d,13]. So far, the computational studies focused on the electronic structure and properties of the nucleophilic phosphinidene complexes [2,11,14] and less on their reactivity, which is part of this study.

Stephan's phosphinidene **1** can be formed from Cp$_2$ZrCl$_2$ by reaction with (a) lithium phosphide to form intermediate **3** through exchange of Cl for PHR followed by elimination of HCl with KH (pathways A and B, Scheme 2) or (b) with an excess of lithium phosphide to replace the chloride of **3** with subsequent exchange of PH$_2$R for PR$_3$ (pathways C and D, Scheme 2). For neither route could the intermediate formation of the 16-electron phosphinidene complex **6** be confirmed experimentally. The only intermediate detected by ^{31}P NMR spectroscopy was zirconium diphosphide complex (**5**, δ 51.6 ppm) when two equivalents of lithium phosphide were used [15]. This diphosphide may undergo intramolecular H-transfer (a) to phosphine-stabilized
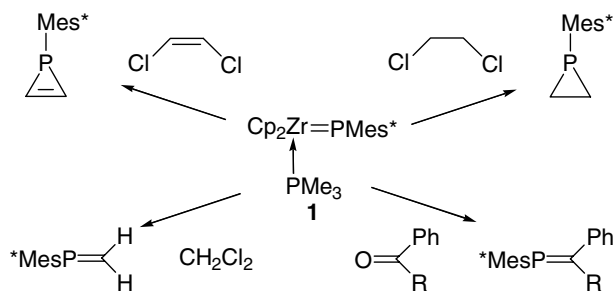
phosphinidene **1*** followed by trimethylphosphine ligand exchange to give **1** (pathway D) or (b) eliminate the ancillary primary phosphine ligand (PH$_2$R) first to form the intermediate 16-electron phosphinidene complex **6** (pathway C). For the reaction of Cp$_2$ZrCl$_2$ with lithium phosphide and potassium hydride a metallohydride intermediate (**4**) has been postulated [10f], based on NMR-data of the reaction of Cp$_2$ZrCl$_2$ with magnesium in the presence of a primary phosphine and KH [16]. Metallohydride intermediate **4** is then presumed to loose H$_2$ to form phosphinidene **1** upon stabilization of **6** with trimethylphosphine. Alternatively, KH may dehydrohalogenate chlorophosphide complex **3**, as experimentally observed for later transition metal complexes [11b,11c,11d,11e]. With density functional theory we will differentiate between the reaction pathways depicted in Scheme 2.

We further explore the reaction of **1** toward 1,2-dichloroethane that gives phosphirane and zirconocene dichloride **2**. A chloride phosphide intermediate (**8**) was postulated for this reaction (Scheme 3) [10f], but the mechanism is unknown. We will evaluate the two transformations for the two simultaneous bond-breaking and bond-forming (σ-metathesis) steps, that is, **7 → 8** and **8 → 2** + phosphirane.

2. Computational details

All DFT calculations have been performed with the parallelized ADF suite of programs, release 2002.03 [17]. Geometry optimizations were carried out with the generalized gradient approximation, using non-local corrections to exchange by Becke [18] and to correlation by Perdew [19] (BP86), including relativistic effects with the Zeroth Order Regular Approximation (ZORA) [20]. The Kohn–Sham MOs were expanded in a large, uncontracted basis set of Slater-type orbitals (STOs), of a triple-ζ + polarization functions quality (ADF basis set IV or TZP), within the frozen-core approximation using a small core for Zr. An auxiliary set of STOs was used to fit the density for the Coulomb-type integrals [17a].

Scheme 1. Reactivity of zirconium phosphinidene (**1**) toward C–Cl and C=O bonds.
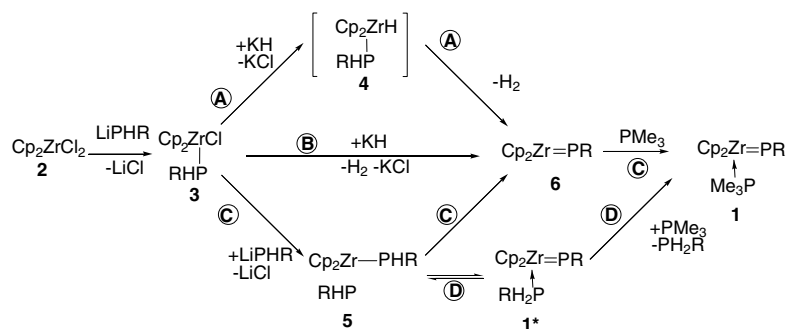
Scheme 2. Pathways for the synthesis of zirconium phosphinidene (**1**).
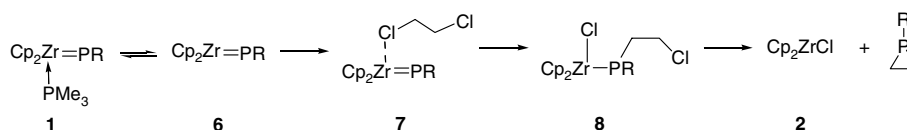
Scheme 3. Formation of phosphirane from zirconium phosphinidene complex **1** and 1,2-dichloroethane.

The nature of the two σ-metathetical transition states (TSs) of the zirconium model complexes was confirmed by the presence of only one imaginary frequency, using B3LYP with a 6-31G* (C, P, H, Cl) basis set and the relativistic LANL2DZ pseudopotentials and basis set for Zr [21], employing the GAUSSIAN 03 suite of programs [22]. For all model complexes considered in this study, Intrinsic Reaction Coordinate (IRC) paths were determined with the ADF program from the approximate Hessian [23] of the optimized transition structures, confirming the connection between the product(s) and the reactant. Solvent effects were estimated by optimizing the geometry within the Conductor-like Screening Model (COSMO) [24,25] with a dielectric constant of $\varepsilon = 4.3$ (diethyl ether). Atomic charges are computed with the Voronoi Deformation Density method, which provides basis-set independent, chemically meaningful charges [17d,26].

^{31}P NMR calculations are calculated with ADF's NMR program [27], using single-point calculations with an all-electron basis for P within the ZORA-approximation on the optimized frozen core structures (vide supra), using PMe₃ as a computational reference for the isotropic shielding (δ −62 ppm with respect to 85% H_3PO_4).

3. Results and discussion

The DFT calculations were performed on model zirconium complexes **1′**–**8′**, the prime indicating that all the phosphorus substituents are replaced for hydrogen atoms. Instead of KH we use LiH as a base for the dehydrohalogenation (**3′** → (**4′** →) **6′**). First, we compare the DFT-computed structures of phosphinidene complex

1′, zirconocene dichloride **2**, zirconocene chloride phosphide **3′**, and zirconocene diphosphide **5′** with available X-ray crystal structure data. Next, we discuss the different reaction pathways from zirconocene dichloride **2** to phosphinidene **1′**. Finally, we explore the phosphinidene's reactivity toward 1,2-dichloroethane.

3.1. Structures

The calculated bond distances and angles of the model structures **1′**, **2**, **3′**, and **5′** are listed in Table 1 together with the reported crystal structure data for $Cp_2(PMe_3)Zr=PMes^*$ (**1**) [10d], Cp_2ZrCl_2 (**2**) [28], $Cp_2ClZr(PHDmp)$ (3-Dmp, Dmp = 2,6-Mes₂Ph) [29], and $Cp_2Zr(PMes_2^*)_2$ (5-Mes*) [30].

The DFT calculated bond distances are in good agreement with the experimental ones. For those between the Zr metal atom and the center of the cyclopentadienyl ring (Zr–Cp) they are slightly longer than in the crystal. This overestimation of M–Cp bond distances by DFT has been observed before [31]. The largest deviation (0.07 Å) is found for the Zr–P bond distance of chlorophosphide **3**. It is known for zirconocene and hafnocene (IV) monophosphide complexes that the M–P (M = metal) bond distance is sensitive to the size of the phosphorus substituent. For instance, Protasiewicz et al. [29]. found the Zr–P bond distance of 2.543 Å for **3**-Mes* [10e] to be almost 0.1 Å longer than in **3**-Dmp (2.639 Å). This was attributed to the competing p-donation of the phosphorus lone pair to complete the Zr 18-electron shell and the reluctance of phosphorus to planarize (Scheme 4). Thus, the Zr–P distance is shorter with a more planar phosphorus atom (sum of angles), which is the case with more bulky substituents. The large Zr–P bond distance (2.710 Å) and small sum

Table 1
Calculated and experimental distances (Å) and angles (°) for **1**$^{(')}$, **2**, **8**$^{(')}$, and **5**$^{(')}$[a]

Bond	1′ (1) [10d]	2 (2) [28]	3′ (3-Dmp) [29]	5′ (5-Mes*) [30]
Zr–Cl	–	2.458 (2.447)[b]	2.449 (2.449)	–
Zr–Cp	2.251[b] (NA)	2.263 (2.202)[b]	2.256[b] (2.193)[b]	2.246[b] (2.214)[b]
Zr=P	2.505 (2.500)	–	–	–
Zr–P	2.682 (2.741)	–	2.710 (2.639)	2.680[b] (2.682)[b]
Cp–Zr–Cp	138.13 (NA)	129.48 (129.51)[b]	131.16 (131.49)	135.88 (131.07)
Cl–Zr–Cl	–	100.59 (97.05)[b]	–	–
P–Zr–P	81.39 (101.4)	–	–	102.15 (97.84)
Cl–Zr–P	–	–	95.15 (97.02)	–

[a] Experimental values are in parentheses.
[b] Average of similar values.
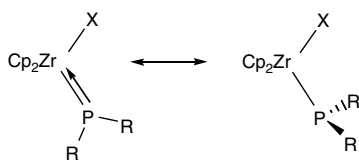
Scheme 4. Competing electronic configurations in zirconocene phosphides.

of phosphorus angles (295.0°) for model complex **3′** (having H-substituents only) is in agreement with this notion. Hence, it is no surprise that the calculated geometry of **3′** deviates slightly from the experimental ones. Using hybrid-DFT calculations Protasiewicz and coworkers [29] estimated that planarization of **3′** would require 6.8 kcal/mol.

Like **3** the influence of the phosphide groups is also apparent in **5**. The two Zr–P bonds are of equal lengths (ca. 2.68 Å) for both **5′** and **5**-Mes* with similar non-planar phosphorus atoms for model **5′** (Σ 290 and 311), but with a nearly flat one for **5**-Mes* (Σ 302 and 356). We assume this difference to be due to inaccuracies in the X-ray crystal structure of **5**-Mes* where the H-atoms occupy calculated positions. However, hafnocene [32] and zirconocene diphosphides [33] with other substituents like **5**-Dmp [29] are reported to have one short M–P bond with a planar phosphorus (Zr: 2.519 Å, Σ 357) and one long bond with a bent phosphorus (Zr: 2.725 Å, Σ 302).

Whereas the calculated Zr bond angles for all models compare well with the experimental structures, the calculated P=Zr–P bond angle of model phosphinidene complex **1′** (81.4°) is a surprising 20° smaller than the experimental one. We attribute this to the absence of steric bulk in the model structure (H instead of mesityl and methyl groups). Also the rather long 2.682 Å Zr–P bond for the stabilizing phosphine group (PMe₃) in **1′** (versus 2.741 Å in **1**) reflects this effect and suggests the ligand to be weakly bound to the metal center.

3.2. Formation of zirconocene phosphinidene complex 1′

The first step in the synthesis is the phosphide substitution of zirconocene dichloride to **3**, which is exothermic by 9.4 kcal/mol and slightly more with the Et₂O-solvent model (13.5 kcal/mol). As discussed above, there are different paths from this intermediate to the phosphinidene complex. Table 2 gives the reaction energies for each of the steps. The minor influence of Et₂O as

solvent is included in this table. Where used in the text these values are given in parentheses.

We start by exploring the dehydrohalogenation with LiH. The formal elimination of HCl (as LiCl and H₂) to give **6′** can occur as a one (Scheme 3, path B) or two-step (path A) process that is slightly endothermic by 6.6 (4.5) kcal/mol, but, of course, is entropy driven by the release of hydrogen. Subsequent complexation with PH₃ to give **1′** gives 22.8 kcal/mol stabilization.

If reaction of **3′** with LiH results in hydride substitution (and elimination of LiCl), zirconium hydride intermediate **4′** should be formed, which is 20.1 kcal/mol exothermic. Consequently, the subsequent elimination of hydrogen is endothermic by 26.7 kcal/mol. Stephan and coworkers [10e,10f] has suggested that the reaction with potassium hydride proceeds in such a stepwise manner based on an observed ³¹P NMR resonance at 37.9 ppm in the reaction of Cp₂*ZrCl₂ with Mg and cyclohexylphosphine that was attributed to Cp₂*Zr(H)(PHCy) [16] because of its similarity with analogous hafnium hydride complexes (δ 30.5–96.3 ppm). Hillhouse and coworkers preferred instead a single step process for the KH promoted dehydrohalogenation of Zr and Hf complexes [34]. This path B finds support in the known synthesis of late transition metals complexes via a dehydrohalogenation pathway [11b,11c,11d,11e].

The argument for the occurrence of **4** is thus based on an observed chemical shift, which we examine now in more detail. Hafnium phosphide hydride complexes of type **4** have low-field ³¹P NMR-chemical shifts compared to the phosphide chloride complexes of type **3** [34]. When this trend is extended to zirconium complexes, the ³¹P NMR nuclei for **4**-cyclohexyl should be *deshielded* as compared to 71.1 ppm for **3**-cyclohexyl [34], which is in contrast to the reported *high-field* resonance at 37.9 ppm for **4**-cyclohexyl. To further elaborate this point we calculated the ³¹P NMR chemical shifts of both **3**-*i*Pr (δ −28 (Hf), 3 (Zr), ppm) and **4**-*i*Pr (δ 80 (Hf), 108 (Zr) ppm), which indeed confirm the low-field resonance for **4** with respect to that of **3**. Even though substituents may influence the pyramidalization at phosphorus and thus the ³¹P NMR chemical shift [29], it seems unlikely that **4**-cyclohexyl has been detected. This may lead to the conclusion that KH simply acts as a base in the dehydrohalogenation reaction **3 → 6** (pathway B, Scheme 2).

Finally, using an excess of lithium phosphide, instead of LiH (or KH), might give intermediate **5′** through a

Table 2
Energies (in kcal/mol) for the reaction steps in the formation of **1′**

	2 → 3′	3′ → 4′	4′ → 6′	3′ → 6′	3′ → 5′	5′ → 1′	5′ → 6′	6′ → 1′
E	−9.4	−20.1	26.7	6.6	−9.2	9.7	32.5	−22.8
E(Et₂O)	−13.5	−20.7	25.2	4.5	−13.1	6.4	30.1	−23.8

second halide–phosphide exchange ($3' \rightarrow 5'$) that is similarly exothermic (9.2 (13.1) kcal/mol) as the first one. Intramolecular H-transfer would then yield phosphine-stabilized phosphinidene $1'$ endothermically (9.7 kcal/mol) with a barrier of 31.6 kcal/mol (path D). Expulsion of the phosphine (PH_3) group to give the 16-electron phosphinidene ($5' \rightarrow 6'$, path C) is unlikely in light of the endothermicity of 32.5 kcal/mol. Reactive phosphinidenes **6** with various P-substituents and Cp-type ligands are suggested as reactive intermediates in the thermal decomposition reactions of diphosphide complexes **5** [15]. The phosphinidene has only been captured with PMe_3 in the case of **6** where R = Mes* and the Cp-ligands on Zr are unsubstituted [10d]. Phosphinidenes **6** are typically suggested to result form direct elimination of a phosphine (path C) [10,15], while H-transfer and ligand exchange (path D) has so far not been considered as an alternative. Because dissociation of PMe_3 from **1** occurs easily and hence also the exchange of phosphine ligands, path D may indeed be the more viable one.

3.3. Reaction of the zirconocene phosphinidene complex with 1,2-dichloroethane

Phosphinidene complex **1** substituted with a supermesityl group is known to react with 1,2-dichloroethane to form the corresponding phosphirane. Chloride–phosphide **8** has been proposed as intermediate [10f], formed from the reaction of the transient phosphinidene **6** with the dichloride (Scheme 5). The by-product of this reaction is Cp_2ZrCl_2 (**2**) from which phosphinidene **1**, in turn, can be resynthesized conveniently as discussed.

We investigated the reaction of 1,2-dichloroethane with model complex $1'$, shown in Scheme 5, where the prime indicates again H-substituents only. Table 3 summarizes relevant structural parameters for the stationary points on the potential energy surface including the two transition structures that are depicted in Fig. 1. Table 4 lists the reaction energies for each of the steps of Scheme 5 and the activation energies for the two C–Cl bond-breaking processes (σ, π-bond metathesis) [35].

The reaction starts by dissociating the phosphine ligand from $1'$. As noted this process requires 22.8 kcal/mol for the model system, but likely less for the mesityl substituted system **1** due to steric repulsion between the auxiliary phosphine and cyclopentadienyl ligands (vide infra). The experimental system is reactive at room temperature [10f,10g,10h].

Table 3
Selected bond distances (in Å) for the stationary points of the reaction of $1'$ with 1,2-dichloroethane

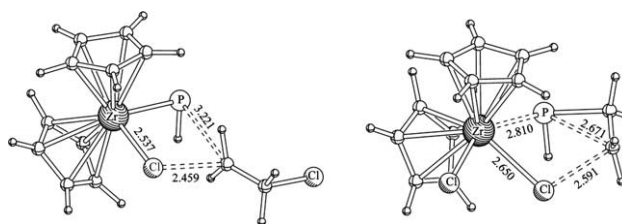| Bond	$1'$	$6'$	$7'$	$TS_{7' \rightarrow 8'}$	$8'$	$TS_{8' \rightarrow 2}$	**2**
Zr–P(=P)	2.500	2.473	2.501	2.596	2.682	2.810	–
Zr–Cl_1	–	–	2.773	2.537	2.451	2.582	2.458
Zr–Cl_2	–	–	–	–	–	2.650	2.458
P–C_1	–	–	–	3.221	1.901	2.002	1.891[a]
P–C_2	–	–	–	–	–	2.671	1.891[a]
C_1–Cl_1	1.823[b]	1.823[b]	1.867	2.459	–	–	–
C_2–Cl_2	1.823[b]	1.823[b]	1.817	1.876	1.829	2.591	–

[a] In phosphirane.
[b] In 1,2-dichloroethane.

Fig. 1. Transition structures for C–Cl bond breaking $TS_{7' \rightarrow 8'}$ (left) and $TS_{8' \rightarrow 2}$.

In $6'$, the Zr–P bond length is shortened by 0.027 Å with respect to $1'$ and more polarized (charges $6'$: Zr +0.345, P −0.308; $1'$: Zr +0.239, P −0.288). The strong Zr=P polarization is also evident from the frontier orbitals of $6'$ with the HOMO consisting for 65% of phosphorus atomic orbitals and the LUMO for ~80% of those of zirconium. The combination of the electron-deficient zirconium center and the nucleophilic phosphorus in [2,11c] makes this species particularly suitable to react with polarized bonds, such as C–Cl and C=O.

One of the chlorine atoms of 1,2-dichloroethane complexes weakly to the electrophilic zirconium center (10.2 (9.5) kcal/mol) of $6'$ to yield precomplex $7'$, with a large Zr–Cl distance of 2.773 Å, and a similar Zr=P distance as in $1'$ (2.501 Å). The high reactivity of phosphinidene intermediate $6'$ is reflected in the very exothermic conversion of complex $7'$ into $8'$ (55.5 (54.5) kcal/mol) and its modest barrier (10.4 (12.5) kcal/mol) that is associated mainly with C–Cl bond cleavage. In the σ,π-metathetical transition structure ($TS_{7' \rightarrow 8'}$, Fig. 1), both the forming Zr–Cl bond (2.537 Å) and the dissociating C–Cl bond (2.459 Å) are product-like, while the Zr–P bond (2.596 Å) is elongated halfway to its final length in $8'$. The developing positive charge on the carbon atom
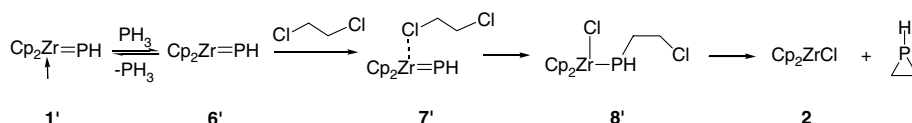
Scheme 5. Formation of phosphirane from zirconium phosphinidene complex $1'$ and 1,2-dichloroethane.

Table 4
Energetics and barriers (in kcal/mol) for the steps in the reaction of $1'$ with 1,2-dichloroethane

	$1' \rightarrow 6'$	$6' + C_2H_4Cl_2 \rightarrow 7'$	$TS_{7' \rightarrow 8'}$	$7' \rightarrow 8'$	$TS_{8' \rightarrow 2}$	$8' \rightarrow 2 + C_2H_5P$
E	22.8	−10.2	10.4	−55.5	30.0	−18.6
E(Et$_2$O)	23.8	−9.5	12.5	−54.5	26.1	−17.2

(+0.014) in the transition structure is stabilized by the lone pair on phosphorus, but P–C bond formation is lagging (3.221 Å). The non-reacting C–Cl bond is elongated by 0.044 Å and the C–C bond shortened by 0.047 Å (with respect to 1,2-dichloroethane), which indicates hyperconjugative stabilization of the electron-deficient β-carbon atom. Structure $8'$ closely resembles $3'$. The phosphorus atom is slightly flatter (Σ 302.2) and the Zr–P bond slightly shorter (Δ 0.03 Å), but these effects are sensitive to the size of the substituent as discussed for 3-Mes* [10e].

The next σ-bond metathesis step that converts $8'$ into zirconocene dichloride 2 and phosphirane is less exothermic (18.6 (17.2) kcal/mol) than the first and has accordingly a higher reaction barrier (30.0 (26.1) kcal/mol). Pre-coordination of the chloride atom to the zirconium center could be identified, only in a *cis* fashion, but this complex was found to be 6.3 kcal/mol less stable than $8'$, which sharply contrasts the stabilizing coordination for first σ-bond metathesis step. In the transition structure, ($TS_{8' \rightarrow 2}$, Fig. 1) both the forming Zr–Cl bond (2.650 Å) and the breaking C–Cl (2.591 Å) bond are again more product-like than the P–C bond (2.671 Å). The Zr–P bond is elongated along each of the steps in the $6' \rightarrow 7' \rightarrow 8'$ sequence, before it is cleaved in the second transition structure (2.810 Å) to render the phosphirane product. IRC-calculations indicate that the phosphirane dissociation occurs simultaneously with σ-bond metathesis.

This outlined mechanism indicates that a labile ligand is essential to generate in situ a highly reactive 16-electron nucleophilic phosphinidene complex, which is an aspect that is also increasingly recognized in the development of active metathesis catalysts [36]. The active phosphinidene complex must further have an adequately polar M=P bond to accommodate a second σ-bond forming step. In this process, the zirconocene is regenerated and can be used again for the synthesis of the phosphinidene complex, thereby offering opportunities for a catalytic cycle.

4. Conclusion

In this density functional theory study, we investigated the formation of zirconocene phosphinidene complex $1'$ from Cp$_2$ZrCl$_2$ using LiH and/or LiPH$_2$. Our aim was to obtain a better mechanistic understanding of the experimentally observed process that uses KH and/or a phosphide with a bulky substituent. Two pathways were

considered, both starting from the initial chloride phosphide complex $3'$. When LiH is used to perform the dehydrohalogenation a phosphine is needed as an auxiliary ligand to stabilize the 16-electron phosphinidene complex $6'$. The dehydrohalogenation likely occurs in a single step and not via phosphide hydride complex $4'$. Calculated ^{31}P NMR chemical shift data for the Zr and Hf complexes in comparison with available experimental data exclude $4'$ as reaction intermediate. With excess lithium phosphide nucleophilic replacement of the chloride substituent of $3'$ is instead more likely. The generated diphosphide $5'$ then undergoes an intramolecular H-transfer to directly afford phosphinidene complex $1'$. This route may lead to other group 6–9 transition metal phosphinidene complexes.

Dissociation of the stabilizing phosphine ligand from $1'$ gives the highly reactive nucleophilic 16-electron phosphinidene complex $6'$ that reacts with 1,2-dichloroethane to phosphirane and ZrCl$_2$ that can be regenerated to the phosphinidene complex. The initial step in this process is coordination of one of the halides to the electron-deficient zirconium center. In the subsequent σ,π-metathesis, C–Cl bond cleavage and P–C bond forming take place in an asynchronous fashion. The resulting intermediate $8'$ undergoes the second asynchronous metathesis step in which the chloride is transferred from carbon to zirconium with simultaneous formation and dissociation of the phosphirane ring. This second step is less exothermic than the first one and also has a higher reaction barrier.

It appears evident that the facile formation of a 16-electron species is the crucial step both in generating the reaction phosphinidene complex and in its reactivity, making the zirconium complex unique.

References

[1] (a) K.B. Dillon, F. Mathey, J.F. Nixon, Phosphorus: the carbon copy, Wiley, Chichester, 1998;

(b) F. Mathey (Ed.), Phosphorus–carbon Heterocyclic Chemistry: the Rise of a New Domain, Pergamon, Amsterdam, 2001;
(c) F. Mathey, N.T. Tran Huy, A. Marinetti, Helv. Chim. Acta 84 (2001) 2938–2957;
(d) K. Lammertsma, M.J.M. Vlaar, Eur. J. Org. Chem. (2002) 1127–1138;
(e) K. Lammertsma, Top. Curr. Chem. 229 (2003) 95–119.

[2] A.W. Ehlers, K. Lammertsma, E.J. Baerends, J. Am. Chem. Soc. 124 (2002) 2831–2838.

[3] G. Frison, F. Mathey, A. Sevin, J. Organomet. Chem. 570 (1998) 225–234.

[4] (a) W.A. Herrmann (Ed.), Complexes Containing Metal/carbon Multiple Bonds in Synthetic Methods of Organometallic and Inorganic Chemistry, Georg Thieme Verlag Stuttgart, New York, 1997;
(b) B. Alcaide, L. Casarrubios, G. Dominguez, M.A. Sierra, Curr. Org. Chem. 2 (1998) 551–574;
(c) K.H. Dötz, P. Tomuschat, Chem. Soc. Rev. 28 (1999) 187–198;
(d) A. de Meijere, H. Schirmer, M. Duetsch, Angew. Chem. 112 (2000) 4124–4162;
A. de Meijere, H. Schirmer, M. Duetsch, Angew. Chem. Int. Ed. 39 (2000) 3964–4002;
(e) J. Barluenga, J. Santamaria, M. Tomas, Chem. Rev. 104 (2004) 2259–2283.

[5] (a) J. Feldman, R.R. Schrock, Prog. Inorg. Chem. 39 (1991) 1–74;
(b) R.R. Schrock, Tetrahedron 55 (1999) 8141–8153;
(c) R.R. Schrock, J. Chem. Soc., Dalton Trans. (2001) 2541–2550;
(d) R.R. Schrock, Chem. Rev. 102 (2002) 145–179.

[6] (a) A. Marinetti, F. Mathey, J. Fischer, A. Mitschler, J. Chem. Soc., Chem. Commun. (1982) 667–668;
(b) A. Marinetti, F. Mathey, J. Fischer, A. Mitschler, J. Am. Chem. Soc. 104 (1982) 4484–4485;
(c) A. Marinetti, F. Mathey, Organometallics 1 (1982) 1488–1492;
(d) A. Marinetti, F. Mathey, Organometallics 3 (1984) 456–461.

[7] (a) J.B.M. Wit, G.T.v. Eijkel, F.J.J.d. Kanter, M. Schakel, A.W. Ehlers, M. Lutz, A.L. Spek, K. Lammertsma, Angew. Chem. 111 (1999) 2716–2719;
J.B.M. Wit, G.T.v. Eijkel, F.J.J.d. Kanter, M. Schakel, A.W. Ehlers, M. Lutz, A.L. Spek, K. Lammertsma, Angew. Chem. Int. Ed. 38 (1999) 2596–2599;
(b) J.B.M. Wit, G.T. van Eijkel, M. Schakel, K. Lammertsma, Tetrahedron 56 (2000) 137–141.

[8] (a) B.T. Sterenberg, K.A. Udachin, A.J. Carty, Organometallics 20 (2001) 2657–2659;
(b) B.T. Sterenberg, A.J. Carty, J. Organomet. Chem. 617-618 (2001) 696–701;
(c) B.T. Sterenberg, K.A. Udachin, A.J. Carty, Organometallics 20 (2001) 4463–4465;
(d) J. Sánchez-Nieves, K.A. Udachin, A.J. Carty, J. Am. Chem. Soc. 125 (2003) 2404–2405;
(e) B.T. Sterenberg, K.A. Udachin, A.J. Carty, Organometallics 22 (2003) 3927–3932.

[9] A.H. Cowley, Acc. Chem. Res. 30 (1997) 445–451 (references cited therein).

[10] (a) Z. Hou, D.W. Stephan, J. Am. Chem. Soc. 114 (1992) 10088–10089;
(b) J. Ho, R.J. Drake, D.W. Stephan, J. Am. Chem. Soc. 115 (1993) 3792–3793;
(c) J. Ho, R.J. Drake, Z. Hou, D.W. Stephan, Organometallics 12 (1993) 3145–3157;
(d) Z. Hou, T.L. Breen, D.W. Stephan, Organometallics 12 (1993) 3158–3167;
(e) J. Ho, R. Rousseau, D.W. Stephan, Organometallics 13 (1994) 1918–1926;
(f) T.L. Breen, D.W. Stephan, J. Am. Chem. Soc. 117 (1995) 11914–11921;

(g) T.L. Breen, D.W. Stephan, J. Am. Chem. Soc. 118 (1996) 4204–4205;
(h) T.L. Breen, D.W. Stephan, Organometallics 15 (1996) 5729–5737;
(i) T.L. Breen, D.W. Stephan, Organometallics 16 (1997) 365–369;
(j) D.W. Stephan, Angew. Chem. 112 (2000) 322–338;
D.W. Stephan, Angew. Chem. Int. Ed. 39 (2000) 314–329.

[11] (a) R. Melenkivitz, D.J. Mindiola, G.L. Hillhouse, J. Am. Chem. Soc. 124 (2002) 3846–3847;
(b) A.T. Termaten, T. Nijbacker, M. Schakel, M. Lutz, A.L. Spek, K. Lammertsma, Organometallics 21 (2002) 3196–3202;
(c) A.T. Termaten, H. Aktas, M. Schakel, A.W. Ehlers, M. Lutz, A.L. Spek, K. Lammertsma, Organometallics 22 (2003) 1827–1834;
(d) A.T. Termaten, T. Nijbacker, M. Schakel, M. Lutz, A.L. Spek, K. Lammertsma, Chem. Eur. J. 9 (2003) 2200–2208;
(e) A.T. Termaten, M. Schakel, A.W. Ehlers, M. Lutz, A.L. Spek, K. Lammertsma, Chem. Eur. J. 9 (2003) 3577–3582.

[12] (a) G. Trinquier, G. Bertrand, Inorg. Chem. 24 (1985) 3842–3856;
(b) D. Gonbeau, G. Pfister-Guillouzo, A. Marinetti, F. Mathey, Inorg. Chem. 24 (1985) 4133–4140;
(c) G. Frison, F. Mathey, A. Sevin, J. Organomet. Chem. 570 (1998) 225–234;
(d) A.W. Ehlers, K. Lammertsma, E.J. Baerends, Organometallics 17 (1998) 2738–2742;
(e) S. Creve, K. Pierloot, M.T. Nguyen, Chem. Phys. Lett. 285 (1998) 429–437;
(f) S. Creve, K. Pierloot, M.T. Nguyen, L.G. Vanquickenborne, Eur. J. Inorg. Chem. (1999) 107–115;
(g) S. Grigoleit, A. Alijah, A.B. Rozhenko, R. Streubel, W.W. Schoeller, J. Organomet. Chem. 643-644 (2002) 223–2230;
(h) K. Lammertsma, A.W. Ehlers, M.L. McKee, J. Am. Chem. Soc. 125 (2003) 14750–14759.

[13] (a) S. Blaurock, E. Hey-Hawkins, Eur. J. Inorg. Chem. (2002) 2975–2984;
(b) S. Blaurock, E. Hey-Hawkins, Z. Anorg. Allg. Chem. 628 (2002) 37–40;
(c) S. Blaurock, E. Hey-Hawkins, Z. Anorg. Allg. Chem. 628 (2002) 2515–2522.

[14] (a) M.T. Benson, T.R. Cundari, Int. J. Quantum Chem. 65 (1997) 987–996;
(b) G. Chung, M.S. Gordon, Organometallics 22 (2003) 42–46.

[15] E. Hey-Hawkins, S. Kurz, J. Organomet. Chem. 479 (1994) 125–133.

[16] J. Ho, D.W. Stephan, Organometallics 10 (1991) 3001–3003.

[17] (a) E.J. Baerends, D.E. Ellis, P. Ros, Chem. Phys. 2 (1973) 41–51;
(b) G. te Velde, E.J. Baerends, J. Comput. Phys. 99 (1992) 84–98;
(c) C. Fonseca-Guerra, O. Visser, J.G. Snijders, G. te Velde, E.J. Baerends, in: METECC-95, E. Clementie, C. Corongiu (Eds.), Cagliari, 1995, pp. 303–395.;
(d) G. te Velde, F.M. Bickelhaupt, E.J. Baerends, C.F. Guerra, S.J.A. van Gisbergen, J.G. Snijders, T. Ziegler, J. Comput. Chem. 22 (2001) 931–967.

[18] A.D. Becke, Phys. Rev. A 38 (1988) 3098–3100.

[19] J.P. Perdew, Phys. Rev. B 33 (1986) 8822–8824.

[20] E. van Lenthe, A.W. Ehlers, E.J. Baerends, J. Chem. Phys. 110 (1999) 8943–8953.

[21] P.J. Hay, W.R. Wadt, J. Chem. Phys. 82 (1985) 270–283.

[22] M.J. Frisch, G.W. Trucks, H.B. Schlegel, G.E. Scuseria, M.A. Robb, J.R. Cheeseman, J.A. Montgomery Jr., T. Vreven, K.N. Kudin, J.C. Burant, J.M. Millam, S.S. Iyengar, J. Tomasi, V. Barone, B. Mennucci, M. Cossi, G. Scalmani, N. Rega, G.A. Petersson, H. Nakatsuji, M. Hada, M. Ehara, K. Toyota, R. Fukuda, J. Hasegawa, M. Ishida, T. Nakajima, Y. Honda, O. Kitao, H. Nakai, M. Klene, X. Li, J.E. Knox, H.P. Hratchian, J.B. Cross, C. Adamo, J. Jaramillo, R. Gomperts, R.E.

Stratmann, O. Yazyev, A.J. Austin, R. Cammi, C. Pomelli, J.W. Ochterski, P.Y. Ayala, K. Morokuma, G.A. Voth, P. Salvador, J.J. Dannenberg, V.G. Zakrzewski, S. Dapprich, A.D. Daniels, M.C. Strain, O. Farkas, D.K. Malick, A.D. Rabuck, K. Raghavachari, J.B. Foresman, J.V. Ortiz, Q. Cui, A.G. Baboul, S. Clifford, J. Cioslowski, B.B. Stefanov, G. Liu, A. Liashenko, P. Piskorz, I. Komaromi, R.L. Martin, D.J. Fox, T. Keith, M.A. Al-Laham, C.Y. Peng, A. Nanayakkara, M. Challacombe, P.M.W. Gill, B. Johnson, W. Chen, M.W. Wong, C. Gonzalez, J.A. Pople, GAUSSIAN 03, Revision B.05, Gaussian, Inc., Pittsburgh, PA, 2003.

[23] Numerical frequencies are computationally very demanding for these large systems.

[24] (a) A. Klamt, G. Schüürmann, J. Chem. Soc. Perkin Trans. 2 (1993) 799–805;
(b) A. Klamt, J. Phys. Chem. 99 (1995) 2224–2235;
(c) A. Klamt, V. Jones, J. Chem. Phys. 105 (1996) 9972–9981;
(d) C.C. Pye, T. Ziegler, Theor. Chem. Acc. 101 (1999) 396–408.

[25] Using radii: P = 1.80, H = 1.20, Li = 1.82, Cl = 1.75, C = 1.70, Zr = 2.38 Å, taken from S.S. Batsanov, J. Mol. Struct. (Theochem.) 468 (1999) 151–159.

[26] C.F. Guerra, J.-W. Handgraaf, E.J. Baerends, F.M. Bickelhaupt, J. Comput. Chem. 25 (2004) 189–210.

[27] G. Schreckenbach, T. Ziegler, J. Phys. Chem. 99 (1995) 606–611.

[28] J.Y. Corey, X.-H. Zhu, L. Brammer, N.P. Rath, Acta Crystallogr. C 51 (1995) 565–567.

[29] E. Urnéžius, S.J. Klippenstein, J.D. Protasiewicz, Inorg. Chim. Acta 297 (2000) 181–190.

[30] E. Hay-Hawkins, S. Kurz, J. Organomet. Chem. 479 (1994) 125–133.

[31] M.J. Mayor-López, J. Weber, Chem. Phys. Lett. 281 (1997) 226–232.

[32] (a) R.T. Baker, J.F. Whitney, S.S. Wreford, Organometallics 2 (1983) 1049–1051;
(b) L. Weber, G. Meine, R. Boese, N. Augart, Organometallics 6 (1987) 2484–2488.

[33] A.-M. Larsonneur, R. Choukroun, J.-C. Daran, T. Cuenca, J.C. Flores, P. Royo, J. Organomet. Chem. 444 (1993) 83–89.

[34] G.A. Vaughan, G.L. Hillhouse, A.L. Rheingold, Organometallics 8 (1989) 1760–1765.

[35] P.W. van Leeuwen, Homogeneous Catalysis: Understanding the Art, Springer, Berlin, 2005, Chapter 2.9.

[36] (a) R.H. Grubbs, S. Chang, Tetrahedron 54 (1998) 4413–4450;
(b) M. Scholl, T.M. Trnka, J.P. Morgan, R.H. Grubbs, Org. Lett. 1 (1999) 953–956;
(c) M. Scholl, T.M. Trnka, J.P. Morgan, R.H. Grubbs, Tetrahedron Lett. 40 (1999) 2247–2250;
(d) J. Huang, E.D. Stevens, S.P. Nolan, J.L. Petersen, J. Am. Chem. Soc. 121 (1999) 2674–2678;
(e) A. Fürstner, Angew. Chem. 112 (2000) 3140–3172;
A. Fürstner, Angew. Chem. Int. Ed. 39 (2000) 3012–3043;
(f) T.M. Trnka, R.H. Grubbs, Acc. Chem. Res. 34 (2001) 18–29;
(g) S.B. Garber, J.S. Kingsbury, B.L. Gray, A.H. Hoveyda, J. Am. Chem. Soc. 122 (2000) 8168–8179.